464 IMPROVING DOWNSLOPE WIND FORECASTS IN A MOUNTAINOUS REGION: ASSESSING UNCERTAINTY IN HIGH- RESOLUTION MODELING OVER THE LAS VEGAS FORECAST ZONE

Andre Pattantyus[a], Sen Chiao[a], Stanley Czyzyk[b]

[a]Florida Institute of Technology, Melbourne, Florida
[b]National Weather Service, Las Vegas, Nevada

1 INTRODUCTION

Severe downslope wind events are widespread across the western United States, often causing surface gustiness and damage on the ground, and clear air turbulence (CAT) for air traffic. With four airports in the greater Las Vegas area, forecasting these transient and dangerous weather events are a major concern for the staff of the Las Vegas National Weather Service Forecast Office. With mountains covering much of the forecast region these events are widespread, however they reach differing strengths due to local topography. Downslope winds were well documented during the Terrain Induced Rotor Experiment (T-REX) in Owens Valley, CA in 2006, also within the forecast region. This study is the first attempt to address the evolution of severe downslope wind events in Las Vegas, NV, as well as to explore the predictability of such severe weather events from the high resolution modeling perspective. Stable boundary conditions will also be simulated in the Owens Valley to investigate formation and structure of the stable boundary layer.

Past theoretical studies suggested the basic dynamics of the severe downslope wind may be categorized into two major theories. The resonant amplification theory was proposed by Clark and Peltier (1984) and the hydraulic theory proposed by Smith (1985). Through idealized experiments Smith (1989) and Vosper (2004) have created thresholds for different mountain wave regimes based on Froude number and non-dimensional parameters. An observational downslope wind study conducted by Colman and Dierking (1992) suggested three necessary criteria are conducive to downslope winds including: 1) an inversion at or just above the ridge top; 2) strong cross-barrier flow near ridge top; 3) cross-barrier flow decreasing with height to a critical level between 3000 and 5500 m MSL. In this study we will examine both theoretical and observational mechanisms of downslope winds in the Las Vegas Valley.

The present study is focused on the development of a suitable model configuration for operational purposes, capable of simulating severe downslope wind events in the Las Vegas Valley. To achieve this end we set out two primary goals: 1) to evaluate the WRF model performance of simulating downslope events with high resolution spatial and topographical data; and 2) to determine the mechanism responsible for the downslope winds and create criteria to assist operational forecasters predict the strength of these events. It is hypothesized that the choice of atmospheric boundary layer schemes will result in significant differences in wind and temperature forecast error below some near surface level.

The developed model grid-spacing configuration was subsequently tested over the Owens Valley, CA, also in the NWS Las Vegas Forecast Zone. This area includes more robust terrain with greater relief which presents a challenge for numerical models, especially at higher horizontal resolutions. Terrain slopes

Corresponding author address: Andre Pattantyus Florida Institute of Technology, Dept. of Marine and Environmental Systems, Melbourne, FL 32901; email: apattantyus2008@my.fit.edu

greater than 30° are known to cause errors in the vertical velocity field shortly after integration begins. The cases being examined are enhanced observing periods (EOPs) 2 and 3 from the T-REX in 2006 and represent more stable conditions. The model appears to forecast the shallow slope flows without being able to explicitly solve them. However, this does present challenges for other surface forecast variables, principally temperature.

2 MESOSCALE AND SYNOPTIC ENVIRONMENTS

Two severe downslope wind events were reported on 15 April 2008 and 4 October 2009 in Las Vegas, NV. Both events evolved from similar large-scale forcing. A surface cold front approached the region from the north/northwest which enhanced a pressure gradient across California as cooler maritime air was blocked by the Sierra Nevada Mountains. This increased local surface winds from the southwest ahead of the front. The 4 October 2009 event was more prolonged due to slow movement of the frontal boundary.

The Aircraft Meteorological Data Reports (AMDAR) sounding from McCarran International Airport Las Vegas at 0525 UTC 15 April 2008 indicated several strong wind shear layers from the surface to around 4000 m (Fig. 1a). The inversion layer was near the same level at this time (Fig. 1b). Subsequently, the inversion layer dropped to near 2700. Maximum sustained winds recorded along the lee slopes of the Spring Mountains during this event were near 25 m s^{-1} with gusts of 30+ m s^{-1}. An AMDAR sounding at 0630 UTC 4 October 2009 showed an inversion near 2700 m (Fig. 1c), while strong low level wind shear was found below that level (Fig. 1d). A subsequent sounding at 1334 UTC revealed the inversion height may have decreased to near 2000 m. At this time there was weaker low level wind shear but very strong shear above the inversion.

Since both events evolved from similar large-scale forcing, the ability to predict these events appears reasonable. However, the 4 October 2009 case continued through a diurnal cycle and experienced changes in intensity resulted in much stronger downslope winds on the lee slopes and stronger gustiness across the Las Vegas Basin at times. The difficulty then becomes the ability to forecast the strength of the event. In order to do this, the key parameter(s) to understanding event intensity must be determined.

Enhanced observing periods (EOPs) 2 and 3 were conducted in Owens Valley, CA in post-frontal, stable conditions from 2300 UTC 29 March to 2000 UTC 20 March 2006 and 2300 UTC 18 April to 2000 UTC 19 April 2006 respectively. Surface analyses from NCEP (not shown) display in both cases a high pressure center is located to the north/northeast of Owens Valley with weak winds in the vicinity of the valley. 500-hPa data (not shown) reveal westerly winds twice as strong during EOP2 then EOP3, which occur just above the peaks of the Sierra Nevada Mountains and affect entrainment within Owens Valley. Further observations for the EOPs will be addressed in the results section.

3 MODEL DESCRIPTION AND EXPERIMENTAL DESIGN

Numerical simulations were performed using the WRF-ARW v3.1. A double-nested simulation was configured with grid spacing of 4.0 km (92 x 84 dimensions) and 1.0 km (201 x 201 dimensions) for domains 1 and 2, respectively. A total of 61 unequally spaced terrain-following vertical levels are employed in which 20 levels are distributed in the lowest 2.0 km in order to sufficiently resolve the atmospheric boundary layer. The lowest level is 11 meters above ground level. Additional vertical configurations were used to assess the necessary resolution in the boundary layer that is required to represent the downslope mechanism. A default vertical configuration was used in which 60 vertical are spaced logarithmically from the surface to 50 hPa (YSU 60). This configuration generated seven levels in the lowest km and two in the lowest 100 m. Another configuration utilizing 137 (YSU 137) vertical levels was also run. The levels were spaced every 50 m through the lowest 2000 m, resulting in only two levels in the lowest 100 m, but nine in the lowest half km. In contrast, the 61 level configuration (YSU 61) generated four levels in the lowest 100 m.The initial and time-dependent lateral boundary conditions are derived from the North American Mesoscale Model (NAM-218, ~12 km grid spacing) forecasts from the National Center for Environmental Prediction. No cumulus scheme was used on either grid and the

Noah Land-surface model was incorporated. The discussions to follow will concentrate on the inner 1.0 km resolution domain results (Fig. 2).

It is widely recognized that the boundary layer schemes may have important effects on the simulation of downslope winds. We evaluate the performance of three ABL schemes in the WRF-ARW model through comparison of surface observations (20 sites) in the Las Vegas valley. These schemes include the Yonsei University (YSU) scheme, Mellor-Yamada Janjic (MYJ) scheme, and Quasi-Normal Scale Elimination (QNSE) scheme. Root mean square errors (RMSE) and bias are calculated. Simulations for the Owns Valley utilized the QNSE scheme since it has been shown to outperform other schemes in simulations of stable boundary layers.

4 MODEL RESULTS

4.1 *Model sensitivity experiments*

Two sets of sensitivity tests were completed during this research in order to develop an adequate operational model configuration. To evaluate which ABL scheme is most adequate, model wind speeds and temperatures are compared to station data for 20 locations for the period 0600 to 2300 UTC 15 April 2008 (Table 1), excluding spin-up time from 0000 to 0600 UTC. The surface temperature bias is calculated to show the cold/warm bias of the model. The surface wind bias is calculated to show the over/under-estimation of the model. Overall, the YSU temperature forecasts have lower bias and RMSE compared to the QNSE and MYJ. Mean wind bias for YSU is significantly higher than the other schemes but has a low RMSE. Separating the four stations with mountain influence from those in the valley reveals stations in the valleys have much lower mean wind bias and RMSE compared to those mountain stations. It is at these valley stations that the YSU shows higher forecast skill. MYJ and QNSE schemes tend to underestimate wind speeds more so than the YSU leading to the higher RMSE. Since this event represents an active weather period where high wind speeds are of great concern, underestimation of wind speeds would not be recommended. Various vertical configurations are also tested. Simulated potential temperature profiles at KLAS for YSU 60, YSU 61, and YSU L137 (not shown) display inversion heights on the order of 2 km, with YSU 60 a bit higher (~2.4 km), a likely result of poor vertical resolution. YSU 137 has a temperature bias that approaches zero but is due to daytime overestimates and lower nocturnal underestimates of temperature. A comparison of model performance of the three configurations from Table 1 reveals that the wind forecasts are considerably better for YSU 61.

4.2 *15 April 2008 Downslope Event*

The high-resolution configuration YSU 61 was applied as the control simulation for the 15 April 2008 event. At 0900 UTC 15 April 2008 strong downslope winds were found along Red Rock Canyon. Flow accelerates from 5 to 20 ms^{-1} as it crosses ridge moves down the lee slope. Trapped gravity waves were also propagating along the base of the Spring Mountains across the Las Vegas Valley, which also implies the occurrence of surface gustiness. The inverse Froude number ($\hat{n}$ = Nh/U) in this case is 2.75 (N = 0.022 s^{-1}, h = 2000 m, $\bar{U}$ ~ 16 ms^{-1}), which is consistent with the production of trapped lee waves and rotors from theoretical studies by Edisvik and Utnes (1997) as well as observations by Mobbs et al. (2005).

To examine the characteristics of the propagating and/or resonant trapped gravity waves, a cross-section of wind (parallel to the cross-section) and vertical velocity fields are constructed along AA' (Fig. 2). Figure 3a shows very strong updrafts (~4 ms^{-1}) present across this region at 1200 UTC 15 April. Amplification of the gravity waves can be seen right above the lee side of the mountain as stronger winds are advected down to the valley floor from over 4 km. It appears lee waves occurred across the Las Vegas Basin, and concentrated from the surface up to 3 km. Two areas of flow reversal (i.e. rotors) are evident across the Las Vegas Basin as well. The simulated, as well as AMDAR, potential temperature profiles confirmed that an inversion layer was present around 2500 m. This result is consistent with the lee wave rotor flow regime suggested by Vosper (2004).

4.3 4 October 2009 Downslope Event

The 4 October 2009 event is chosen as a comparison to the 15 April 2008 event because it was observed to be more prolonged event of similar intensity. The 4 October event is longer in duration due to the slow movement of the cold front, allowing the cross-barrier gradient to be maintained over a longer time period. The longevity of this October event also means that it will be affected by the diurnal evolution of the ABL, an investigation into which now be addressed.

Strong winds (10 ms^{-1}) are found across the ridge of Spring Mountain Range around 0000 UTC 4 October 2009. One hour later, a train of mountain-generated gravity waves is extended across the Las Vegas Basin. Inspection of cross-section BB' (Fig. 2), oriented along axis of mean flow, reveals the nature of the mountain waves (Fig. 3b). The AMDAR sounding from KLAS indicates a region of limited wind shear from the surface to about 3600 m at 0000 UTC 4 October (Fig. 1d), below the inversion near 4000 m (Fig. 1c). Subsequently, a transition from mountain waves to trapped lee waves begins as inversion heights decreased around 0600 UTC 4 October, resulting in trapped lee waves on the Las Vegas basin below the inversion. Inversion height is lower than 3000 m at 0800 UTC. Subsequently, the area of maximum winds (>20 ms^{-1}) extends from the mountain ridge down the lee slopes (Fig. 3c). Overall, the inverse Froude number ($\hat{h}$) here was 1.7 (N = .017 s^{-1}, $\bar{U}$ = 20 ms^{-1}), supporting lee waves with modulated turbulence intensity near the, while F_i ~ 0.70 also suggested the lee waves with the occurrence of rotors not likely (e.g., Fig. 9 in Vosper 2004).

4.4 Owens Valley, Stable Boundary Layer Cases

Fernando and Weil (2010) noted that the present understanding of the stable boundary layer is poor and different turbulence parameterizations are likely necessary in non-homogenous terrain. The intent was to explore the nocturnal boundary layer development via slope and valley flow dynamics. The same model grid-spacing was applied to the Owens Valley for two cases from the T-REX 2006 field project that represented stable conditions. The QNSE boundary layer scheme was used in these simulations due to its previous performance with stable conditions. However, this configuration was limited in the vertical by the apparent extreme relief of the Sierra Nevada and Inyo Mountains. This limitation removed any explicit solving in the surface and lower boundary layers but did not appear to greatly affect the model results, except for limiting the direct calculation of surface temperatures, which cannot be inferred from similarity theory.

4.4.1 Enhanced Observing Period 2 (EOP2)

EOP2 took place from 2300 UTC 29 March to 2000 UTC 30 March 2006 and was distinguished by a three-layer flow structure within the valley. This was initially thought to be an anti-wind circulation but further analysis revealed the structure to result from external forcing over the lower Inyo and White Mountains to the east (Schmidli et al. 2009, Pattantyus 2010).

The atmospheric boundary layer structure was well documented through soundings approximately every 1.5 h at Independence, CA (Fig. 4). Boundary layer depth began near the height of the Sierra Nevada Range and decreased overnight as detrainment and cold pool formation progressed. The temperature profiles indicated a conditionally stable environment which became more stable as the surface cold pool formed. Estimates of the depth of the cold pool are ~100 m. The effects of this on mixing within the boundary layer can be seen in the vertical velocity fields in figure 5. Stronger vertical motions are found near the valley slopes and above the temperature inversion. The motions near the slopes are associated with the nocturnal downslope flows, while the upper level motions are associated with detrainment from the vertical wind sheer and mixing at the top of boundary layer. The layered flow structure also follows the vertical velocities pattern. Slope flows dominate the surface layer, with a transition to valley flow above this in the residual layer. Exchange between the layers is implied by the vertical velocities. Moisture appeared to be entrained from the surface layer to the residual layer. The externally forced flow layer (southerly flow near 3000 m) also shows large vertical velocities at 06 UTC in the boundary with the valley flow but these do not persist as the external flow grows in strength. Further analysis of virtual potential temperature profiles as well as flux tower data will

reveal the extent of mixing and exchange between layers.

Model vertical resolution near the surface was found to be severely limited by the terrain around the Owens Valley. The lowest vertical level was at a height of 102 m above the ground, which meant that all surface flows were not explicitly solved but resulted from similarity theory in the boundary layer scheme. Overall, there is good agreement between observations and the model for stations across the valley throughout the event. However, there is no relation for surface air temperature in QNSE scheme similarity theory making it challenging to forecast this variable given model results.

4.4.2 EOP 3

EOP3 was similar to EOP2 but the overlying synoptic forcing was weaker, leading to a more stable boundary layer developing from 2300 UTC 18 April to 2000 UTC 19 April 2006. In addition to the weaker synoptic flow, the lack of snow cover, and hence soil moisture, resulted in a much dryer surface layer, and less moisture flux into the nocturnal boundary layer.

Profiles from Independence, CA for EOP3 (Fig. 6) show this very stable boundary layer structure. Temperature inversions are initially 1000 m lower, wind speeds are half at strong throughout the boundary layer, but relative humidity is roughly the same as in EOP2 at the surface, however changes little with height. This is the case with subsequent soundings, implying little mixing within the boundary layer. Mixing seemed to occur in the surface layer after sunrise as the stronger up-valley winds pushed speeds up to 10 ms^{-1}. Only the 0209 UTC sounding has adequate boundary layer resolution and shows a cold pool depth of nearly 100 m. Lack of resolution in subsequent soundings near the surface does not allow for an estimate of the maximum cold pool depth in this case.

The low wind environment is seen in the cross-section plots in figure 7 as well. There are also low values of vertical velocity throughout much of the valley and free atmosphere, since wind shear is relatively low. In this plot however, there is a noticeable divergence from surface observations. Observed wind directions are from the east for much of the period, whereas the model predicts westerly winds at the surface. This appears to be an issue in the model's ability to predict the overall weak synoptic environment.

5 CONCLUSIONS

Two severe downslope wind events affecting the Las Vegas Basin were investigated in this paper using the Weather Research and Forecasting (WRF) model. The WRF simulated both the 15 April 2008 and 4 October 2009 severe downslope wind events well via high resolution topographical data and high spatial resolution in a two-domain nested setting. The model did well to capture the onset and development of the events, with slight overestimation of wind speeds especially at higher elevations. However, this overestimation seemed to match the station reports of surface wind gusts well. The evolution of the 4 October 2009 through an entire diurnal cycle, shown by the model was supported by linear wave theory. During these events, the model recreated AMDAR data very well, which validated quality of the AMDAR data and performance of the model.

Atmospheric boundary layer (ABL) schemes were tested to determine which most adequate representation of the 15 April 2008 event. Statistics calculated for the ABL schemes revealed that the MYJ and QNSE tended to underestimate valley wind speeds, while the YSU slightly overestimated. The surface wind fields for the schemes showed large differences in surface wind fields, as hypothesized.

The use of higher vertical resolution in the boundary layer greatly improved the surface wind forecast from the default run. The lowest level for the default configuration is ~20 m. The configuration with increased resolution (L137) throughout the model did not produce a more accurate wind forecast than the default (L60), with a lowest model height of almost 30 m. L137 did however, produce higher daytime temperatures than those observed, which artificially lowered its RMSE.

This research highlights the sensitivity of flow over mountains to a number of variables. Boundary layer height appears the most critical factor affecting the type of flow/wave regime that will form. Other factors include wind speed, stability, and inversion strength. Nevertheless,

long-term verifications of model performance are still needed.

Simulations of stable boundary layers in Owens Valley, CA produced impressive results. Vertical resolution in the boundary layer was severely limited by the robust terrain relief but parameterizations of surface processes still produced slope and valley flows that agreed well in most cases with observations. Further investigations are ongoing into the turbulent scales and processes responsible for the mixing between the surface and residual layers. Also future work to improve vertical resolution in the boundary layer over extremely complex terrain is necessary.

6 ACKNOWLEDGEMENTS

This research was supported by the UCAR/COMET partners project (S09- 75798) and partly by the Grant W911NF-09-1-0441 from the US Army Research Office. Thanks to NCAR CISL for computing resources. T-REX data provided by NCAR/EOL under NSF sponsorship.

7 REFERENCES

Clark, T. L., and W. R. Peltier, 1984: Critical level reflection and the resonant growth of nonlinear mountain waves. *J. Atmos. Sci.,* **41**, 3122-3124.

Clark, T. L., W. D. Hall, and R. M. Banta, 1994: Two-and three-dimensional simulations of the 9 January 1989 severe Boulder windstorm: Comparison with observations. *J. Atmos. Sci.,* **51**, 2317-2343.

Colman, B., and C. Dierking, 1992: The Taku Wind of Southeast Alaska - Its Identification and Prediction, *Weather Forecast.,***7**, 49-64.

Edisvik, K. H., and T. Utnes, 1997: Flow separation and hydraulic transitions over hills modeled by the Reynolds equations. *J. Wind Eng. Ind. Aerody.*, **67-68**, 403-413.

Fernando, H. J. S. and J. C. Weil, 2010: Whither the Stable Boundary Layer? Bull. Am. Meteorol. Soc., **91,** 1475-1484.

Mobbs S. D., and Coauthors 2005: Observations of downslope winds and rotors in the Falkland Islands. *Quart. J. Roy. Meteor. Soc.*, **131**, 329–351.

Pattantyus, A., 2010: Numerical investigation of mountain flows in the Las Vegas and Owens Valleys. Thesis, Department of Marine and Environmental Systems, Florida Institute of Technology, 92 pp.

Schmidli, J., G.S. Poulos, M.H. Daniels, and F.T. Chow, 2009: External influences on nocturnal thermally driven flows in a deep valley. *J. Appl. Meteorol. Climatol*., **48**, 3-23.

Smith, R. B., 1985: On severe downslope winds. *J. Atmos. Sci.,* **42**, 2597-2603.

Smith, R. B., 1989: Hydrostatic Airflow over Mountains. *Adv. Geophys.*, **31**, 1-41

Vosper, S. B., 2004: Inversion effects on mountain lee waves. *Quart. J. Roy. Meteor. Soc.,* **130**, 1723-1748.

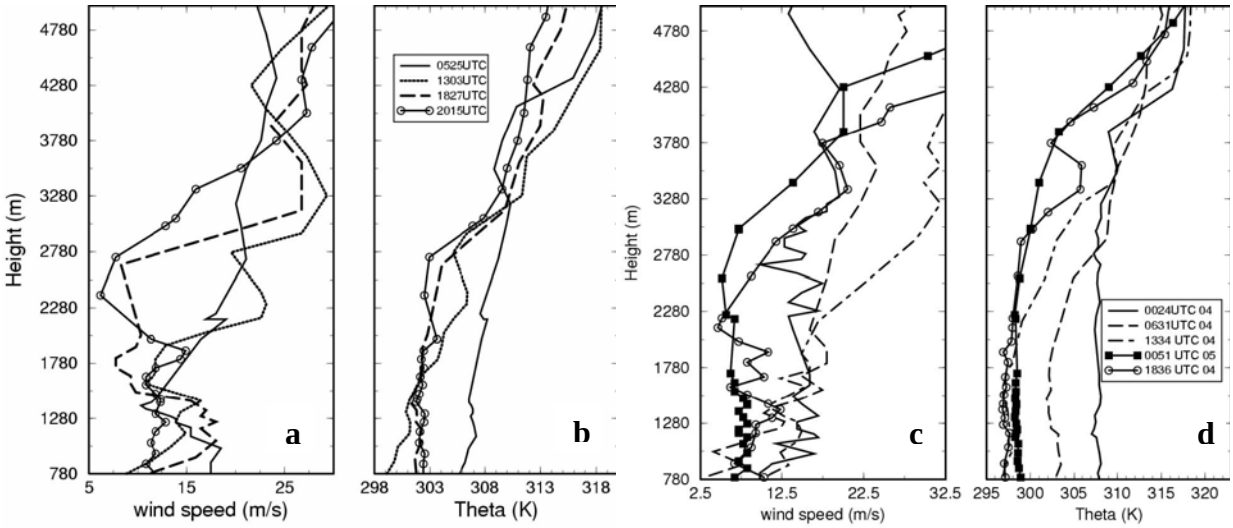

Figure 1: KLAS AMDAR profiles of (a, c) wind speed and (b, d) potential temperature valid 15 April 2008 and 4-5 October 2009 respectively.

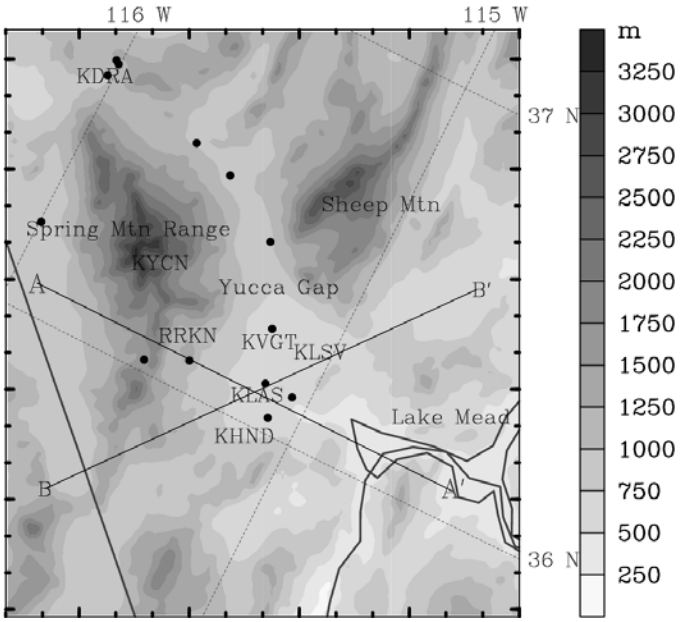

Figure 2: Nested 1 km resolution domain showing Las Vegas area topography, stations for model verification, and cross- sections used to analyze model results

All Stations (20)				
	Temperature		Wind Speed	
Model Run ID	Mean Bias	RMSE	Mean Bias	RMSE
YSU 60 levels	-2.24	2.51	3.83	5.70
QSNE 61 levels	-2.44	2.65	0.48	4.21
YSU 61 levels	-2.18	2.46	1.47	4.12
MYJ 61 levels	-2.57	2.83	0.63	4.09
YSU 137 levels	0.09	1.87	3.63	5.70
Valley Stations (16)				
	Temperature		Wind Speed	
Model Run ID	Mean Bias	RMSE	Mean Bias	RMSE
YSU 60 levels	-2.17	2.46	2.74	4.73
QSNE 61 levels	-2.44	2.65	-0.27	4.14
YSU 61 levels	-2.09	2.37	0.68	3.98
MYJ 61 levels	-2.57	2.83	-0.05	4.05
YSU 137 levels	0.29	1.89	2.71	4.76
Mountain Stations (4)				
	Temperature		Wind Speed	
Model Run ID	Mean Bias	RMSE	Mean Bias	RMSE
YSU 60 levels	-2.50	2.70	7.92	9.33
QSNE 61 levels	-2.46	2.66	3.31	5.97
YSU 61 levels	-2.56	2.80	4.44	6.11
MYJ 61 levels	-2.59	2.82	3.20	5.79
YSU 137 levels	-0.73	1.79	7.11	9.22

Table 1: Statistics from model output values and surface station observations for 06-23 UTC 15 April 2008.

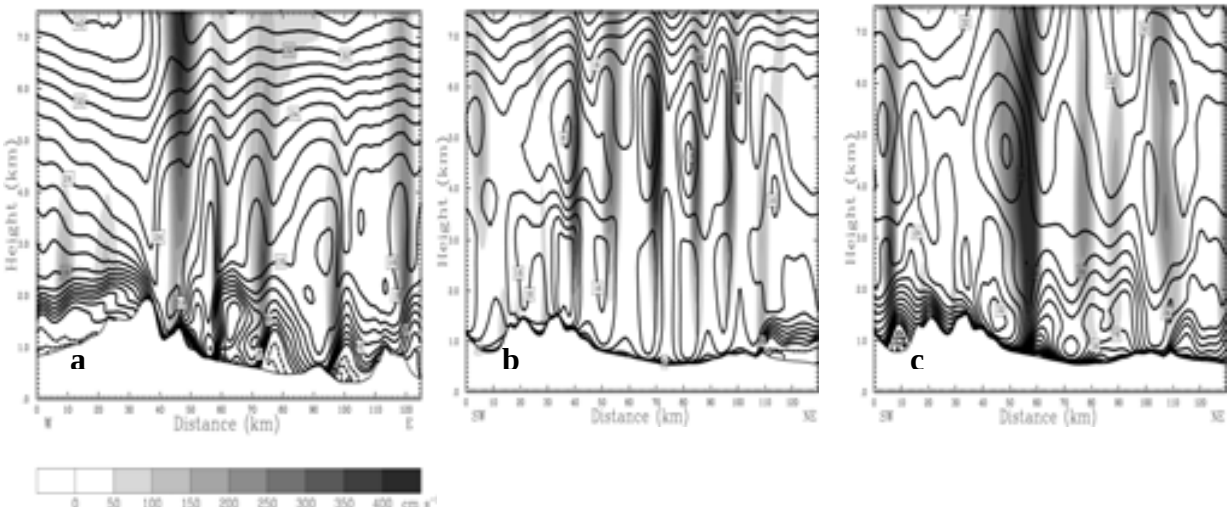

Figure 3: Cross-sections of vertical velocity (shaded) and horizontal wind (contours) valid (a) 12 UTC 15 April 2008, (b) 00 UTC and (c) 12 UTC 4 October 2009.

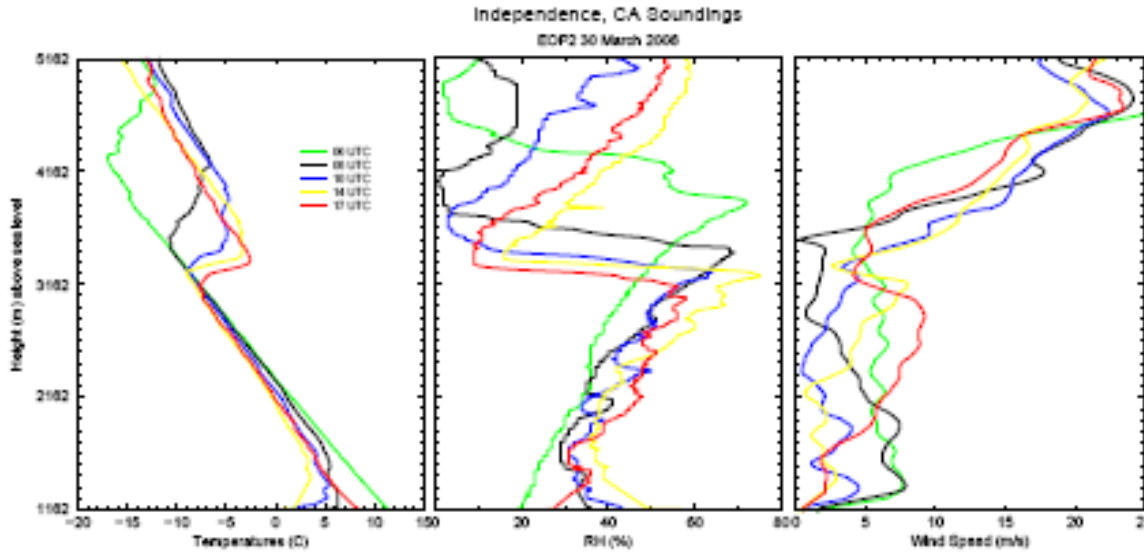

Figure 4: Temperature (°C), RH (%), and wind speed (m/s) profiles from Independence, CA valid 30 March 2006.

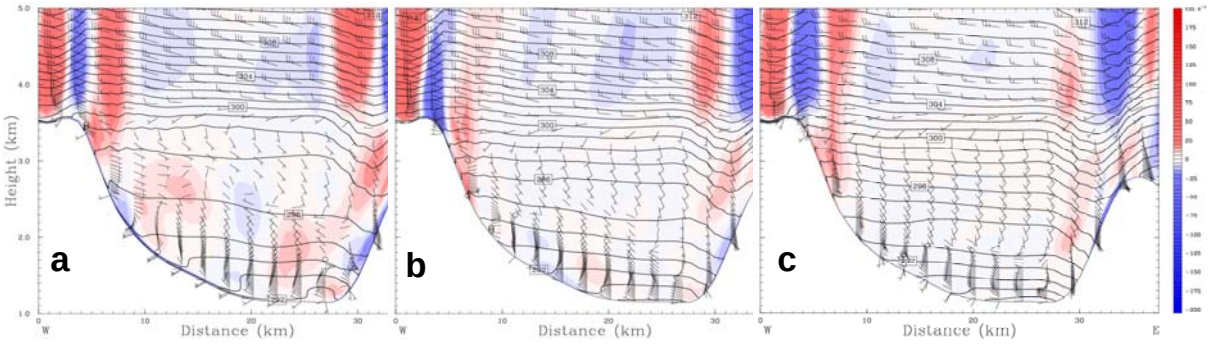

Figure 5: Cross-sections of model horizontal wind (barbs), virtual potential temperature (contours) and vertical velocity (shaded) across Owens Valley valid (a) 06 UTC, (b) 10 UTC, and (c) 14 UTC 30 March 2006.

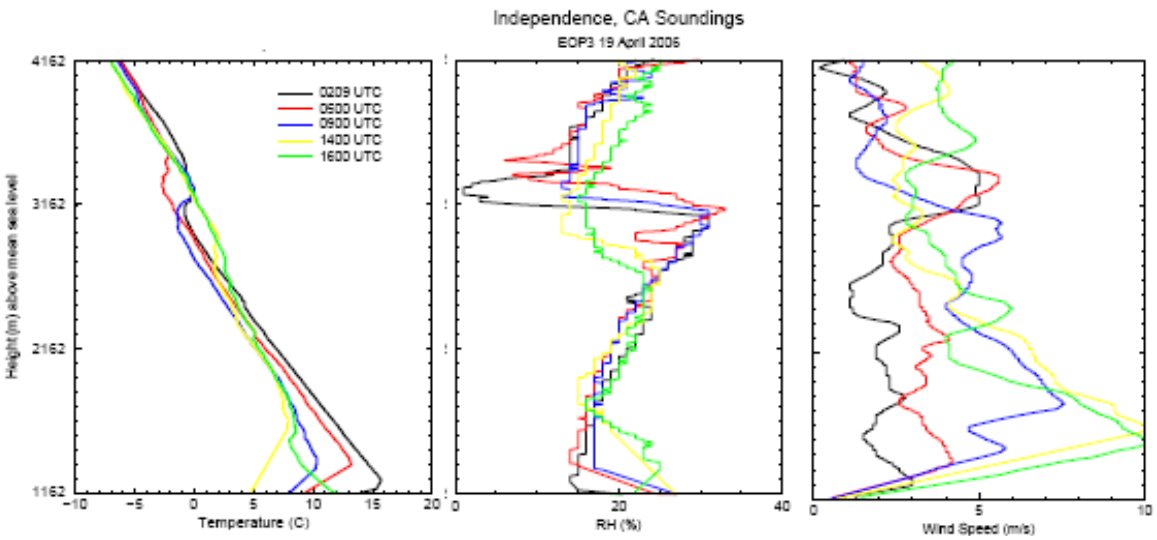

Figure 6: As in Fig. 4, valid 19 April 2006.

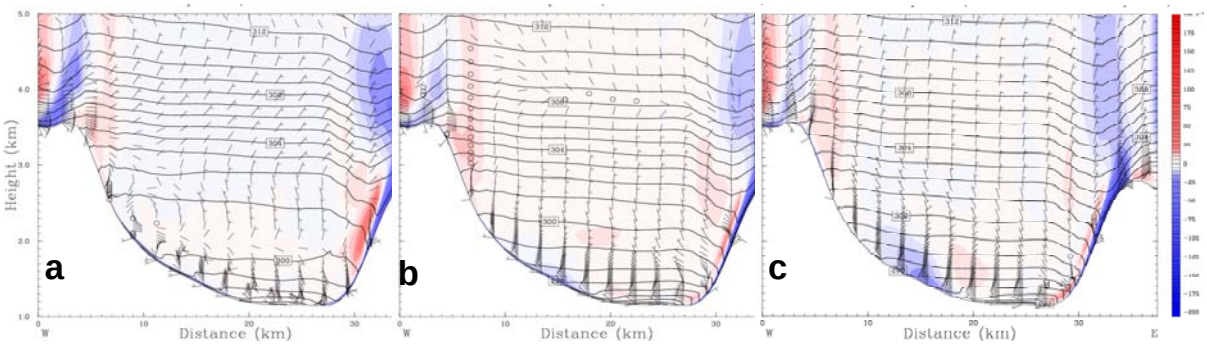

Figure 7: Same as Fig. 5. Valid (a) 06 UTC, (b) 09 UTC, and (c) 14 UTC 19 April 2006.